Efficient low-brightness-pumped Raman amplification of a single high-order Bessel-mode in 335-m of 70-µm-diameter silica-core step-index fiber

SHENG ZHU,[1,*] YUTONG FENG,[1] PRANABESH BARUA,[1,2] AND JOHAN NILSSON[1]

[1]Optoelectronics Research Centre, University of Southampton, Southampton, SO17 1BJ, UK
[2]Currently with SPI Lasers Limited, 6 Wellington Park, Toolbar way, Hedge End, Southampton, SO30 2QU, UK
*Corresponding author: Zhu.S@soton.ac.uk

Received XX Month XXXX; revised XX Month, XXXX; accepted XX Month XXXX; posted XX Month XXXX (Doc. ID XXXXX); published XX Month XXXX

We experimentally demonstrate Raman amplification of signal pulses in a high-order Bessel mode (LP_{06}) at a wavelength of 1121 nm in a 335-m step-index fiber with a 70-µm diameter, 0.227-NA pure-silica core. This was pumped by 5-ns multimode pulses at 1065 nm from an Yb-doped fiber MOPA. The mode purity of the amplified pulses is well preserved to 23 dB of average-power gain, to 774 W of peak power in 2 ns pulses at 20 kHz repetition rate, when pumped with a peak power of 942 W. The pump depletion as averaged over the signal pulses reaches 59%. We believe that this is the first demonstration of stable mode propagation and Raman amplification of a single Bessel-like higher order mode in a fiber of hundreds of meters. This shows the potential for efficient power scaling of a single signal mode with low-brightness pumping, comparable with that from continuous-wave multimode diode lasers. © 2020 Optical Society of America

http://dx.doi.org/10.1364/OL.99.099999

Power scaling and pump-to-signal brightness enhancement in fiber Raman amplifiers (FRAs) are hampered by possible cascaded stimulated Raman scattering (SRS) beyond the targeted Raman Stokes order. In case of cladding-pumping, which converts a multimode pump into a higher-brightness signal in the core, this limits the pump-to-signal area ratio and range of powers for high pump depletion and efficiency, especially for 1st-order operation [1,2]. A large signal waveguide helps, and in the limit of unity area ratio, an alternative to cladding-pumping is to launch the multimode pump into a large multimode core that also guides the signal. Various approaches are used to maintain single-mode signal operation and thus maximize signal brightness (i.e., power per mode) in large cores, mostly targeting the fundamental mode [3–6]. Alternatively, a single higher-order mode (HOM) can also propagate stably in large-core fibers, notably Bessel-like LP_{0m} modes with m≥4 [7]. Rare-earth-based as well as Raman-based fiber amplifiers for HOMs have been demonstrated with brightness enhancement and high mode purity [8,9]. Particularly, FRAs enjoy wavelength agility [10], ubiquitous and low-cost gain medium, better control of fiber perturbations and non-local gain saturation [9]. Previously, we have demonstrated 18 dB Raman amplification of a single HOM in a large mode area fiber with a 50-µm diameter, 0.22-NA, core. The fiber was short, 9 m, thus pulse-pumped by a relatively complex Yb-doped fiber (YDF) source to reach the instantaneous pump brightness and intensity required for Raman amplification in a short fiber. The pump depletion reached 37%, as weighted by the signal pulse shape.

It is now possible to pump Raman gain fibers (RGFs) directly with multimode diode lasers (DLs) [11,12], where long (e.g., 0.1 – 1 km) low-loss fibers and recent improvements in DL brightness (though still relatively low) overcome the weak nature of SRS even continuous-wave (CW). Output power of over 100 W has been demonstrated [13]. The possibility of pumping with multiple DLs wavelength-combined over a narrow [12] or wide [14,15] span alleviate the brightness required of a single DL and may allow for significant further power-scaling. Often, graded-index fibers are used, which favor the Stokes beam in the fundamental mode and improve the Stokes beam quality (the beam cleanup effect) [16], and thus the brightness from pump to signal [17]. Mode-selective launch and feedback with fiber Bragg gratings are other routes to high beam quality and mode purity, but large-core fibers longer than 100 m make mode-coupling a major concern.

Here, we demonstrate Raman amplification of a high-purity LP_{06} mode at 1121 nm with multimode pumping in a 335-m-long fiber with a pure-silica step-index core with diameter of 70 µm and NA 0.227. The effective area of LP_{06} becomes 1110 µm^2. The average-power gain reaches 23 dB with 774 W signal peak power and 942 W pump peak power. At this gain level, the weighted pump depletion is about 59%. The increase in power per mode from pump to signal is estimated to 16 dB. This confirms that FRAs can reach high mode purity and brightness enhancement in long, large-core fibers, even at high gain and conversion efficiency. We attribute this to the high homogeneity in refractive index and

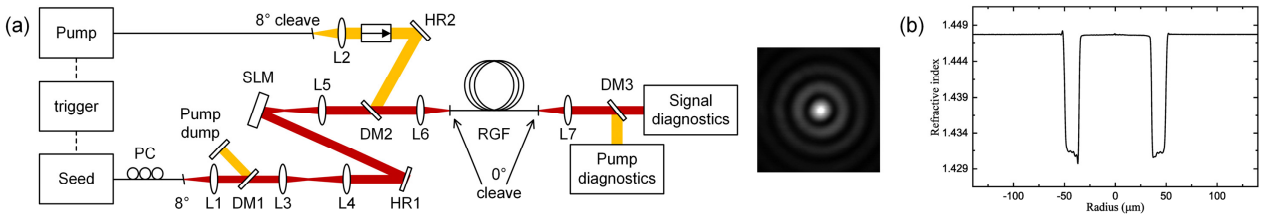

Fig. 1. (a) Schematic diagram of experimental setup with image of the intensity profile at the focal plane after the SLM. (b) Refractive index profile of the RGF. The data is scaled from the measured profile of a 50-μm core fiber pulled from the same preform due to limitations in measurement device.

geometry expected in our fiber, and / or the lack of local gain saturation of Raman amplification. Although we pumped with a pulsed YDF source, these fiber and pump parameters are compatible with CW wavelength-combined DLs, and a single-wavelength DL may suffice with longer fibers. Thus, our results open for power-scaling of CW fiber Raman amplifiers operating on a pure HOM, pumped directly by diode lasers.

Figure 1 illustrates the four main parts of our experimental setup. The pump source (indicated in the top-left corner) is a pulsed master-oscillator power amplifier (MOPA) consisting of a seeding DL (LD1, LC96A1060-20R, Oclaro) and three cladding-pumped fiber amplifiers. LD1 emits up to 1 W peak power at ~1065 nm with 3-dB bandwidth of 3 nm. It is modulated by a 4 GSa/s, 729-MHz bandwidth arbitrary waveform generator (AWG710, Tektronix) via a drive board (BFS-VRM 03 HP, Picolas) to produce optical pulses with ~5 ns duration and 20 kHz repetition rate. The final amplifier comprises a 0.8-m-long commercial YDF (DCF-Yb-50/400P-FA, CorActive) with 50/400 μm core/cladding diameter and 0.13 core NA. This was co-directionally pumped by three 975-nm DLs (PLD-70-975-WS, IPG). The generated pump pulses can reach more than 300 μJ of energy and 60 kW of peak power, which is much higher than needed to pump the RGF. The output beam is collimated by an aspheric lens (L2, f=11 mm) and combined with the Raman seed by a dichroic mirror (DM) before being launched into the RGF. The incident pump beam has an M^2-value of ~7. The focusing half-angle of ~0.1 rad underfills the RGF's NA. For the Raman seed, an 1121-nm FBG-stabilized DL (QFBGLD-1122-400, QPhotonics) emits polarized seed pulses, synchronized with the pump pulses at 20 kHz. The DL is directly modulated by a driver board (BFS-VRM 03 LP, Picolas) which is triggered by a digital delay generator (DG645, Stanford Research Systems). The pulses become ~40 ns, which is long enough to ensure wavelength locking. These pulses are then Raman-amplified in 35 m of single-mode passive fiber (1060XP, Nufern). This incorporates a polarization controller (PC) and is pumped by synchronized 2-ns pulses from an amplified directly modulated 1065-nm DL. Following amplification, the Raman seed pulses have a central wavelength of 1121.2 nm with ~0.16 nm 3-dB bandwidth. Their duration of ~2 ns is determined by the pump pulse duration. The seed pulses are then collimated by an aspheric lens L1 (C240TMC, Thorlabs, f = 8 mm), passed through a DM that blocks residual 1065 nm light and expanded to ~3.2 mm diameter by a pair of plano-convex lenses, L3 (f = 75 mm) and L4 (f = 200 mm), before being sent to a reflective spatial light modulator (SLM-100, Santec). A computer-generated hologram that incorporates the phase profile of an axicon and a diffraction grating converts the incident Gaussian beam into a Bessel beam in the first diffraction order. The incident beam is linearly polarized and aligned by the PC to the preferred polarization of the SLM. The generated diffraction-grating pattern has a fringe spacing of ~88.9 μm and implements an axicon angle of ~0.45° (apex angle 179.55°), selected to match the spatial frequency of LP_{06} in the RGF [18]. The angle can be adjusted to excite different HOMs.

After the SLM, the Raman seed pulses are re-collimated by a plano-convex lens (L5, f=200 mm), combined with the pump pulses in DM2 and launched into the FRA in the center of the setup through DM2. Together with L5, another aspheric lens (L6, f=6.24 mm) images the focal plane of the Bessel-Gauss beam generated by the SLM onto the facet of the RGF to excite the LP_{06} mode. The 335-m RGF is pulled in-house from a commercial preform (Fluosil Preform SWS6.95/SWU1.4, Heraeus). It has a pure-silica core with an NA of 0.227 defined by a fluorine-doped trench. Its refractive index profile is shown in Fig. 1(b). At 1121 nm, the effective-index difference between LP_{06} and its nearest neighbors LP_{16}, LP_{05}, and LP_{07} becomes around 5.0×10^{-4}, 8.9×10^{-4}, and 1.1×10^{-3}. This large difference (an order-of-magnitude larger than that between LP_{01} and LP_{11}) helps to suppress nearest-neighbor mode-coupling, which can otherwise be strong. The gain fiber is coiled on a 31-cm diameter bobbin and has both ends perpendicularly cleaved to minimize beam distortion. The background loss at both 1065 nm and 1121 nm is measured to ~0.8 dB/km and the effective length is hence ~325 m. Raman seed pulses of about 8.5 nJ energy and 2.9 W peak power (estimated from the transmitted average power and fiber loss) are launched into the RGF, together with the pump. The launch efficiency becomes ~69% (signal) and ~50% (pump). The temporal overlap between the pump and signal pulses is carefully adjusted by tuning the delay between the three synchronized drive units to achieve maximum average-power signal gain.

The output beam is collimated by an aspheric lens L7 (f=11 mm, A397-C, Thorlabs) and separated into pump and signal by a DM for their respective diagnostics, in the final, right part of the setup in Fig. 1 (a). The temporal traces of both beams are captured separately by two 12.5 GHz InGaAs detectors (ET-3500, EOT) connected to a 6-GHz oscilloscope (Infiniium 54855A, Agilent). The transmitted pump and signal power are measured, respectively, by a thermal power meter and by a lightwave multimeter (HP 81525A power head connected to HP 8153A module). Optical spectra and intensity profiles are measured by an optical spectrum analyzer (AQ6317B, Ando) in CW measurement mode and two silicon cameras (DCC1545M, Thorlabs).

Fig. 2 shows the average-power gain (i.e., the ratio between the launched and output average powers) *vs.* the launched pump peak

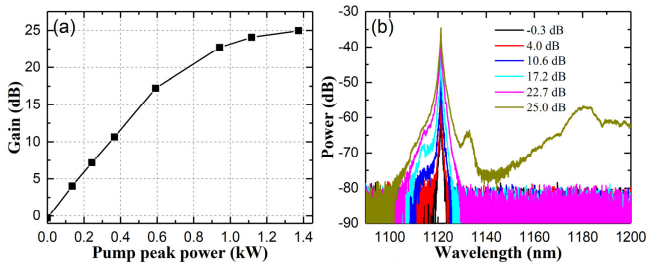

Fig. 2. (a) Measured average-power gain, including all modes. (b) Measured optical spectra of the output signal after the DM at different levels of average-power gain. OSA resolution is 0.1 nm.

power as well as spectra of the amplified signal. The launched power is estimated from the transmitted power and the background loss. The launched pump peak power is calculated from the measured transmitted average pump power when no Raman seed is present, and the FWHM pulse duration of ~11 ns. As the pump power increases, the average-power gain increases almost linearly up to ~17 dB, after which it rolls off, which we attribute to pump depletion. Accounting for the broadening of the pump pulses along the fiber as well as the background loss, the linear growth of Raman gain before depletion corresponds to a Raman gain coefficient of ~54 fm/W, if the pump is evenly distributed across the core. This agrees with the value for pure silica. At 23 dB gain, the launched pump peak power is 942 W and the transmitted signal peak power is 774 W with pulse energy of 1.69 μJ. With higher pump power, the average power gain can be scaled to ~25 dB. However, as shown in Fig. 2 (b), the spectra start to broaden due to nonlinear effects such as self-phase modulation (SPM), and 2nd-order Stokes at ~1180 nm can be seen. Note that the short-wavelength part of the spectra shown is attenuated by the DM that separates the signal and pump. The Raman seed source emits light at 1180 nm which is ~20 dB larger than the quantum fluctuations. Therefore, it is possible that a higher spectral purity of the seed allows for a higher gain before unwanted nonlinear scattering occurs.

Figure 3 shows the temporal traces of selected incident and transmitted signal and pump pulses. In Fig. 3(a), the two solid curves show the transmitted pump pulse at 23-dB signal amplification and the pulse at the same pump power with the seed blocked. The weighted pump depletion is calculated to be ~59.2% by weighing the instantaneous depletion given by $\eta_P(t) = (P_P^{in}(t) - P_P^{out}(t)) / P_P^{in}(t)$ with the instantaneous signal output power [9]. Thus, $\eta_{depletion} = \int P_S^{out}(t)\eta_P(t)dt \Big/ \int P_S^{out}(t)dt$, where P_P^{in}, P_P^{out}, P_S^{out} are output pump without Raman seed, output pump with Raman seed, and output signal power, respectively. Dispersion lengthens the transmitted pump pulse to ~11 ns, from 5 ns at input. The pulse broadening is ~1/3 of the ~20 ns estimated from the core-cladding index difference of the RGF [19], which can be partly explained by the under-filling of the NA by the launched pump and mode-coupling, which counteract dispersion. Even if LP_{06} sees little coupling, other pump modes may be more affected. As shown in Fig. 3(b), the transmitted signal pulses, both unamplified and amplified, have durations of ~2.1 ns, compared to ~2.0 ns on incidence. The amplified signal pulses see a minor shoulder in the leading edge. This is indicative of a small fraction of power in other modes with smaller group index, as a

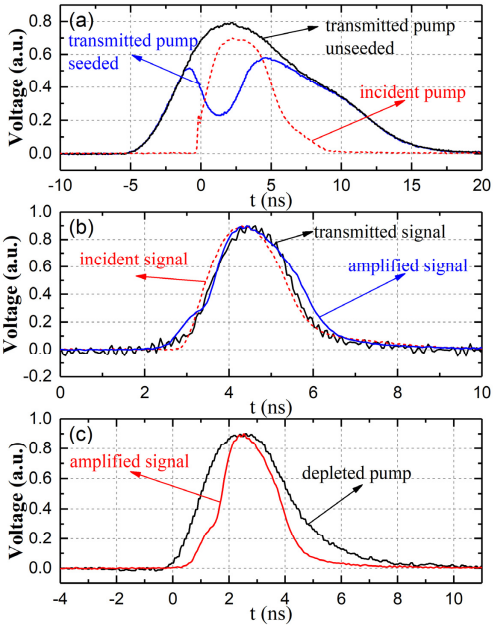

Fig. 3. (a) Measured transmitted pump pulse at 23-dB average-power amplification (solid blue curve) and the transmitted pump pulse at the same pump level with the Raman seed blocked (solid black curve). The incident pump pulse is also shown, but temporally shifted and with different scaling. (b) Measured incident (dashed red curve) and transmitted signal pulses at 0 dB (solid black curve) and 23 dB gain (solid blue curve). The traces are scaled to the same height. (c) Pump depletion (black curve) and transmitted signal (red curve) at 23 dB gain. The curves are scaled vertically and shifted temporally so that their peaks coincide.

result of imperfect signal mode excitation and / or minor mode coupling. There is also walk-off between the signal and pump, which can affect the signal pulse shape as well as the pump depletion. As shown in Fig. 3(c), the depleted pump (calculated by subtracting the two pump traces in Fig. 3(a)) is longer than the signal. This is caused by dispersion over the part of the fiber with significant depletion. Note also that the 1-ns walk-off calculated between LP_{06} and $LP_{06\pm1}$ is too small to cause significantly different temporal overlap between a signal in those modes and the pump.

Images of the spatial intensities as well as line profiles through the center of the beam at different gain levels are shown in Fig. 4. Despite a much longer fiber with larger core, the output beams have better contrast between the neighboring maxima and minima than our results in [9] for a 9-m fiber with a 50-μm-diameter core, thanks to the improved incident Bessel beam generated by the SLM over the axicon. The mode remains well preserved with only minor degradation up to 23 dB gain. The slightly elliptical central peaks persist throughout the amplification starting from 0 dB gain and can be seen in the beam incident to the RGF. At 25 dB gain, the contrast between the adjacent maxima and minima decreases, indicating a degraded mode purity. At this gain, the weighted pump depletion reaches ~77%. This could be caused by spatially dependent pump depletion. However, the transverse distribution of the transmitted pump has not been altered significantly, as shown in Fig. 5. The relative spatial depletion, calculated by weighing the difference between seeded and unseeded pump intensities over the unseeded intensity, show little transverse hole burning at both 23 dB and 25 dB gain. Also, the

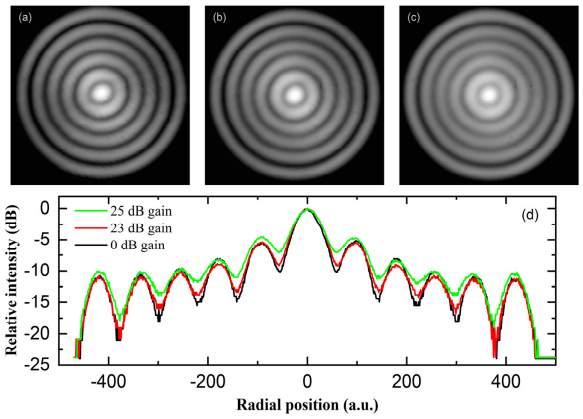

Fig. 4. Intensity profiles in log scale and normalized of output signal beams at (a) 0 dB, (b) 23 dB and (c) 25 dB. (d) Normalized intensity line profiles (in log scale) across the beam center in the horizontal axis at gain level of 0 dB (black curve), 23 dB (red curve) and 25 dB (green curve). Data is recorded with a silicon camera.

thermal load is too small to affect the beam. An alternative possibility is that SRS into 2nd-order Stokes or other nonlinear effects, as evidenced by Fig. 2(b), degrades the purity.

The M^2-value of the incident pump beam corresponds to 49 modes, so at 59% conversion, assuming 90% of the signal power in a single mode, the power per mode becomes ~16 dB higher in the signal than in the pump.

The un-depleted output pump has a central peak nearly twice as high as the average, which boosts the gain for Bessel-modes relative to that of other modes. This is quantified by the pump's overlap with LP_{06}, or the effective area. For uniform pump distribution, this equals the core area (3848 μm^2), but shrinks to 2863 μm^2 for the un-depleted pump distribution. The LP_{06}-gain thus increases by 34%, which is significant but modest. We measured similar gain for the neighboring $LP_{06\pm1}$-modes, but with slightly worse mode purity.

An important attraction of a long fiber is that it allows for pumping with comparatively low brightness, including that available from multimode DLs. The RGF used in this experiment has a beam parameter product (BPP) of ~8 mm·mrad. This can allow for over 90% launch efficiency from a typical DL with ~7.9 mm·mrad BPP (105-μm core delivery fiber with 90% of the power within 0.15 rad half-angle divergence). Although the Raman gain coefficient is significantly lower than with high germanium-doping, and the LP_{06} gain with the pump distribution in our experiments is ~34% higher than with uniform distribution, by scaling the RGF length to 1 km, one can still expect ~15 dB gain with ~200 W of DL pump power. Diode-pumping results [15] with a pure-silica-core support these predictions.

In conclusion, we have demonstrated Raman amplification of LP_{06} mode in 335 m of step-index fiber with 70 μm core diameter with minimal mode distortion up to 23 dB average power gain. The weighted pump depletion reaches 59%. The HOM is excited by a free-space Bessel beam that is converted by an SLM. The Raman gain is limited mainly by higher order Stokes. With a longer RGF and further optimization, pumping with low brightness sources such as diode lasers can be feasible, which opens for a new regime of power scaling and brightness enhancement with clean and stable HOMs.

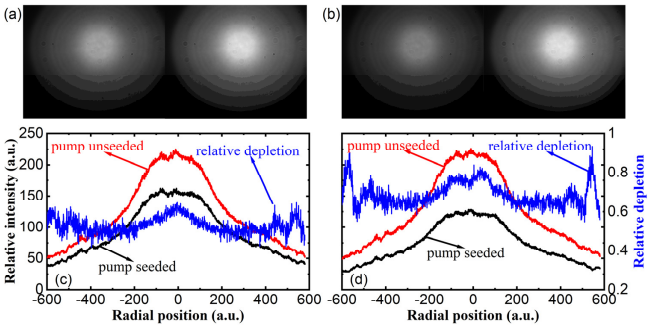

Fig. 5. Intensity images of output pump beams with (left) and without (right) Raman seed at 23 dB (a) and 25 dB (b) gain. Line profiles of output pump beam (left scale) and transverse pump depletion (right scale) are shown at gains of 23 dB (c) and 25 dB (d). Intensity images and line profiles are in linear scale.

Funding. AFOSR (FA9550-14-1-0382).

Acknowledgment. We thank Dr Christophe Codemard for helpful discussions. Sheng Zhu thanks the China Scholarship Council for financial support. Reported data is available from University of Southampton at https://doi.org/10.5258/SOTON/D1498.

Disclosures. The authors declare no conflicts of interest.

REFERENCES

1. J. Ji, Ph.D. dissertation (University of Southampton, 2011)
2. J. E. Heebner, A. K. Sridharan, J. W. Dawson, M. J. Messerly, P. H. Pax, M. Y. Shverdin, R. J. Beach, and C. P. J. Barty, Opt. Express **18**, 14705 (2010)
3. Martin E. Fermann, Opt. Lett. **23**, 52-54 (1998)
4. Y. Jeong, J. K. Sahu, D. N. Payne, and J. Nilsson, Opt. Express **12**, 6088 (2004).
5. L. Dong, H. A. Mckay, A. Marcinkevicius, L. Fu, J. Li, B. K. Thomas, and M. E. Fermann, J. Lightwave Technol. **27**, 1565–1570 (2009).
6. D. Jain, Y. Jung, M. Nunez-Velazquez, and J. K. Sahu, Opt. Express **22**, 31078 (2014).
7. S. Ramachandran, J. W. Nicholson, S. Ghalmi, M. F. Yan, P. Wisk, E. Monberg, and F. V Dimarcello, Opt. Lett. **31**, 1797–1799 (2006).
8. J. W. Nicholson, J. M. Fini, A. M. DeSantolo, E. Monberg, F. DiMarcello, J. Fleming, C. Headley, D. J. DiGiovanni, S. Ghalmi, and S. Ramachandran, Opt. Express **18**, 17651 (2010).
9. S. Zhu, S. Pidishety, Y. Feng, S. Hong, J. Demas, R. Sidharthan, S. Yoo, S. Ramachandran, B. Srinivasan, and J. Nilsson, Opt. Express **26**, 23295 (2018).
10. V. R. Supradeepa, Y. Feng, and J. W. Nicholson, J. Opt. **19**, 023001 (2017).
11. S. I. Kablukov, E. I. Dontsova, E. A. Zlobina, I. N. Nemov, A. A. Vlasov, and S. A. Babin, Laser Phys. Lett. **10**, 085103 (2013).
12. T. Yao, A. Harish, J. Sahu, and J. Nilsson, Appl. Sci. **5**, 1323–1336 (2015).
13. Y. Glick, V. Fromzel, J. Zhang, N. Ter-Gabrielyan, and M. Dubinskii, Appl. Opt. **56**, B97 (2017).
14. N. Zhao, S. Hong, A. V. Harish, Y. Feng, and J. Nilsson, Opt. Eng. **58**, 1 (2019).
15. S. Hong, Y. Feng, and J. Nilsson, IEEE Photon. Technol. Lett. **31**, 1995–1998 (2019).
16. N. B. Terry, T. G. Alley, and T. H. Russell, Opt. Express **15**, 17509 (2007).
17. A. G. Kuznetsov, S. I. Kablukov, A. A. Wolf, I. N. Nemov, V. A. Tyrtyshnyy, D. V Myasnikov, and S. A. Babin, Laser Phys. Lett. **16**, 105102 (2019).
18. J. Demas, L. Rishøj, and S. Ramachandran, Opt. Express **23**, 28531 (2015).
19. J. Ji, C. A. Codemard, J. K. Sahu, and J. Nilsson, Opt. Fiber Technol. **16**, 428–441 (2010).

Full REFERENCES

1. J. Ji, "Cladding-pumped Raman fibre laser sources," Ph.D. dissertation (University of Southampton, 2011).
2. J. E. Heebner, A. K. Sridharan, J. W. Dawson, M. J. Messerly, P. H. Pax, M. Y. Shverdin, R. J. Beach, and C. P. J. Barty, "High brightness, quantum-defect-limited conversion efficiency in cladding-pumped Raman fiber amplifiers and oscillators," Opt. Express **18**, 14705 (2010).
3. Martin E. Fermann, "Single-mode excitation of multimode fibers with ultrashort pulses," Opt. Lett. **23**, 52-54 (1998)
4. Y. Jeong, J. K. Sahu, D. N. Payne, and J. Nilsson, "Ytterbium-doped large-core fiber laser with 1.36 kW continuous-wave output power," Opt. Express **12**, 6088 (2004).
5. L. Dong, H. A. Mckay, A. Marcinkevicius, L. Fu, J. Li, B. K. Thomas, and M. E. Fermann, "Extending Effective Area of Fundamental Mode in Optical Fibers," J. Lightwave Technol. **27**, 1565–1570 (2009).
6. D. Jain, Y. Jung, M. Nunez-Velazquez, and J. K. Sahu, "Extending single mode performance of all-solid large-mode-area single trench fiber," Opt. Express **22**, 31078 (2014).
7. S. Ramachandran, J. W. Nicholson, S. Ghalmi, M. F. Yan, P. Wisk, E. Monberg, and F. V Dimarcello, "Light propagation with ultralarge modal areas in optical fibers.," Opt. Lett. **31**, 1797–1799 (2006).
8. J. W. Nicholson, J. M. Fini, A. M. DeSantolo, E. Monberg, F. DiMarcello, J. Fleming, C. Headley, D. J. DiGiovanni, S. Ghalmi, and S. Ramachandran, "A higher-order-mode Erbium-doped-fiber amplifier," Opt. Express **18**, 17651 (2010).
9. S. Zhu, S. Pidishety, Y. Feng, S. Hong, J. Demas, R. Sidharthan, S. Yoo, S. Ramachandran, B. Srinivasan, and J. Nilsson, "Multimode-pumped Raman amplification of a higher order mode in a large mode area fiber," Opt. Express **26**, 23295 (2018).
10. V. R. Supradeepa, Y. Feng, and J. W. Nicholson, "Raman fiber lasers," J. Opt. 19, 023001 (2017).
11. S. I. Kablukov, E. I. Dontsova, E. A. Zlobina, I. N. Nemov, A. A. Vlasov, and S. A. Babin, "An LD-pumped Raman fiber laser operating below 1 μm," Laser Phys. Lett. **10**, 085103 (2013).
12. T. Yao, A. Harish, J. Sahu, and J. Nilsson, "High-Power Continuous-Wave Directly-Diode-Pumped Fiber Raman Lasers," Appl. Sci. **5**, 1323–1336 (2015).
13. Y. Glick, V. Fromzel, J. Zhang, N. Ter-Gabrielyan, and M. Dubinskii, "High-efficiency, 154 W CW, diode-pumped Raman fiber laser with brightness enhancement," Appl. Opt. **56**, B97 (2017).
14. N. Zhao, S. Hong, A. V. Harish, Y. Feng, and J. Nilsson, "Simulations of multiwavelength cladding pumping of high-power fiber Raman amplifiers," Opt. Eng. **58**, 1 (2019).
15. S. Hong, Y. Feng, and J. Nilsson, "Wide-Span Multi-Wavelength High-Power Diode-Laser Pumping of Fiber Raman Laser," IEEE Photon. Technol. Lett. **31**, 1995–1998 (2019).
16. N. B. Terry, T. G. Alley, and T. H. Russell, "An explanation of SRS beam cleanup in graded-index fibers and the absence of SRS beam cleanup in step-index fibers," Opt. Express **15**, 17509 (2007).
17. A. G. Kuznetsov, S. I. Kablukov, A. A. Wolf, I. N. Nemov, V. A. Tyrtyshnyy, D. V Myasnikov, and S. A. Babin, "976 nm all-fiber Raman laser with high beam quality at multimode laser diode pumping," Laser Phys. Lett. **16**, 105102 (2019).
18. J. Demas, L. Rishøj, and S. Ramachandran, "Free-space beam shaping for precise control and conversion of modes in optical fiber," Opt. Express **23**, 28531 (2015).
19. J. Ji, C. A. Codemard, J. K. Sahu, and J. Nilsson, "Design, performance, and limitations of fibers for cladding-pumped Raman lasers," Opt. Fiber Technol. **16**, 428–441 (2010).